Application of UnSWAN for wave hindcasting in the Dutch Wadden Sea

Marcel Zijlema[‡]

Environmental Fluid Mechanics Section
Faculty of Civil Engineering and Geosciences
Delft University of Technology
P.O. Box 5048
2600 GA Delft, The Netherlands

1 Introduction

While spectral wave models (WAM, WAVEWATCH III and SWAN) mainly focus on large-scale wind-wave and wave-wave interactions, wave features on small scale associated with irregular bathymetry, e.g. surf breaking, triad and wave-current interactions, are critical to understanding wave dynamics and assessing impacts of engineering activities. This is particularly important in the surf zones. An example is a tidal inlet, which is the focus of the present paper.

The Dutch Wadden Sea in the northern part of the Netherlands is a tidal inlet system that is partly sheltered from the North Sea by islands; see Fig. 1. Waves entering a tidal inlet from the open sea and subsequently propagating over tidal shoals vary substantially in length scales. In addition, the Wadden Sea is a particularly challenging area due to its complex bathymetry and the occurrence of many physical processes, such as depth-induced wave breaking, local wave generation and wave-current interaction. All these processes can be characterised as spectral evolution of the wind waves and swells.

Although the quality of the wave height prediction in a tidal inlet is quite good, the prediction of the wave periods and of the spectra is generally poor. As a result, the SBW (Strength and Loads on Water Defenses) project is being carried out for the Dutch goverment (Groeneweg et al., 2009; Van Vledder et al., 2009). In Groeneweg et al. (2009), recently obtained measured data have been used in extensive hindcasts of the tidal inlet of the island Ameland in the Wadden Sea for a variety of storms. These hindcasts were carried out using SWAN (Booij et al., 1999) and provided useful insight in the performance of SWAN and in the relevant processes in the Wadden Sea. For instance, the penetration of low-frequency wave energy over the ebb-tidal delta appears to be significantly underestimated, whereas the computed wave heights in the shallow interior with a nearly horizontal bathymetry are too low compared to the measured ones. Therefore, there is a strong need for accurate and efficient spectral wave simulations to better understand and analyse the interactions between wind, waves and currents in tidal inlets.

2 Use of unstructured grids in terascale environment

The SWAN simulations of Groeneweg et al. (2009) were performed on two curvi-linear grids. The first is a coarse grid covering a large part of the Wadden Sea. The second grid is a detailed one covering the tidal inlet of Ameland and was obtained from refining a part of the larger grid. The resolution in this inlet is about 30 to 50m. See Fig. 2. As reported in Van Vledder et al. (2009), the resulted detailed grid is not optimal, as it is still unnecessarily fine in some areas in the computational domain. Offshore wave boundary conditions for the fine grid were obtained from the coarse grid computation combined with some measured spectra; see Fig. 2. This amounts to the application of an interpolation procedure from coarse to fine grids. Although interpolation is not conceptually difficult, it is a disadvantage because it is costly to perform. The nested mesh is also detrimental because it introduces additional boundaries. Problems often occur

[‡]E-mail: m.zijlema@tudelft.nl

Figure 1: Map of the Dutch Wadden Sea located in the north of the Netherlands, with the inlet of Ameland (source: Google Maps).

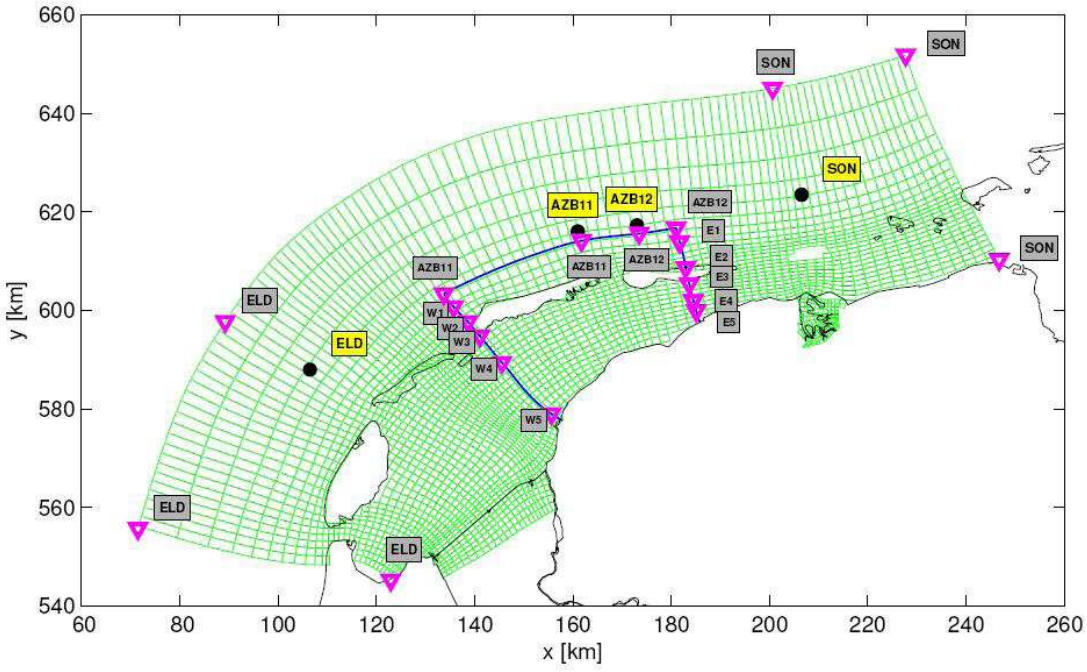

Figure 2: Curvi-linear grid (every fourth grid cell is shown) and outline of the detailed grid, covering the tidal inlet of Ameland (courtesy of Deltares, The Netherlands). The triangles indicate the locations where boundary conditions are imposed, the circles some buoy locations.

near model boundaries, due to mismatches in numerics and/or physics. Different accuracy properties or abruptly local changes in physics can make it difficult to apply the solution from one (coarse) grid as a boundary condition in another (fine) grid.

This static, one-way nested refinement approach is an example of a classic trade-off that is experienced in coastal environmental problems. Better physics require better resolution, but that resolution can be costly. Hence, one must choose a level of resolution that captures the important physics without sacrificing computational efficiency.

Unstructured meshes with variable resolution provide the capability to simultaneously capture scales ranging many orders of magnitude, e.g. from hundreds of kilometers to tens of meters. These meshes concentrate computational effort where it is most needed. Moreover, they offer a very large geometrical flexibility. The application of unstructured grids to the study of wave dynamics in oceanic and coastal areas is a new and powerful technique. For a structured-grid wave model to yield results of the same accuracy, there is no doubt that the computational cost would be much higher.

Recently, an unstructured-mesh version of SWAN has been developed, called UnSWAN (Zijlema, 2009). UnSWAN maintains the structured-grid SWAN versions feature of being unconditionally stable. This is accomplished through the implementation of the unstructured-mesh analog to the four-direction Gauss-Seidel iteration technique that is employed in the structured-grid version. The UnSWAN model orders the mesh vertices in such a way that it can sweep through them and update the action density using updated information from neighboring vertices. It then sweeps through the mesh in opposite directions until the wave energy has propagated sufficiently through geographical space. Thus, this model retains the physics and numerics and the code structure of the structured-grid SWAN model, but is able to run on unstructured meshes. UnSWAN has been verified and validated through its application in many benchmark cases of the so-called ONR testbed (Ris et al., 2002).

In order to efficiently carry out high-resolution simulations with UnSWAN, a parallel code is build using message passing paradigm and tested on a commodity computer cluster. In parallelizing UnSWAN, we employ the same paradigms for high-performance computing as applied in the circulation model ADCIRC (Westerink et al., 2008). In this way, UnSWAN takes advantage of the same scalability as ADCIRC, which remains efficient to thousands of computational processors.

Gains in efficiency create opportunities for rapid benefits in accuracy. Thus, once the set up of the model for the Wadden Sea has proven to be efficient and scalable, the next step will be verification. We will need to learn how best to employ the parameterizations for the source terms to simulate storm waves. Finally, when we are confident that the model is running efficiently and correctly, then we can proceed to validation studies. The work presented here builds on the study of Groeneweg et al. (2009) and seeks to achieve higher accuracy.

3 Model set up

This section presents the set up of the model, including the optimal mesh, the storm instants studied, the hydrodynamic and boundary conditions and the SWAN source term settings.

3.1 Mesh

The first ingredient of the numerical calculations is the design of the unstructured mesh. The tidal inlet and the inner-tidal area require a fine mesh whereas in the open sea in the north a coarse grid is sufficient. This highly variable resolution is reflected by a typically sudden and large change in wave height due to surf breaking on the ebb-tidal delta and regeneration by wind over the inner shoals in front of the mainland. We use the BatTri package (Bilgili and Smith, 2003) to generate the appropriate mesh for the present simulations. This final mesh is depicted in Fig. 3. The mesh is made up of triangles only. As a result, the finest grid resolution is about 15m in between the islands Terschelling (left) and Ameland (right) whereas the coarsest part is about 1,000m. The total number of mesh nodes is 140,703 with many of them located in the tidal inlet and behind the islands.

In order to take advantage of parallel computing, the global mesh is partitioned into local meshes attributed to each of the processors of a distributed-memory machine. For this, the METIS domain-decomposition algorithm has been applied (Karypis and Kumar, 1998). An example of the partition of the mesh on 16 processors is shown in Fig. 3. The local meshes are shown in separate colors, and the processors communicate via the so-called halo layer of overlapping cells that connect these local meshes. The parallel implementation of UnSWAN requires communication only at the nodes of the halo layer along the boundaries of the local meshes.

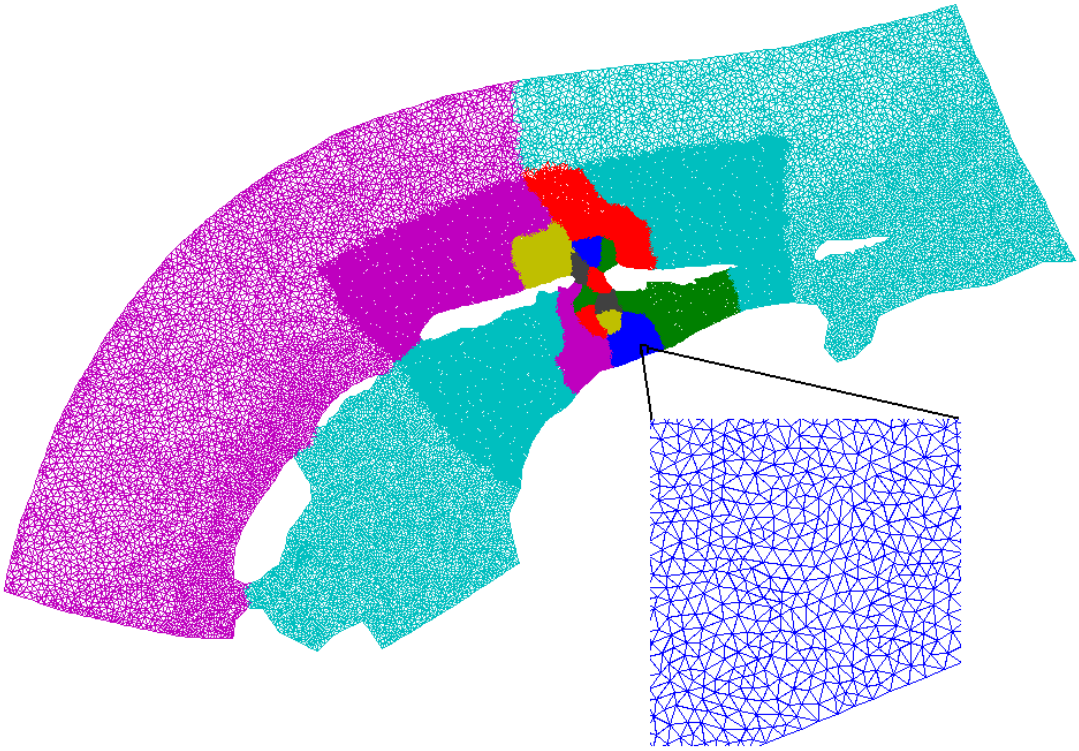

Figure 3: Load-balanced partitioned unstructured mesh of 279,845 triangles of sizes comprized between 15m and 1km.

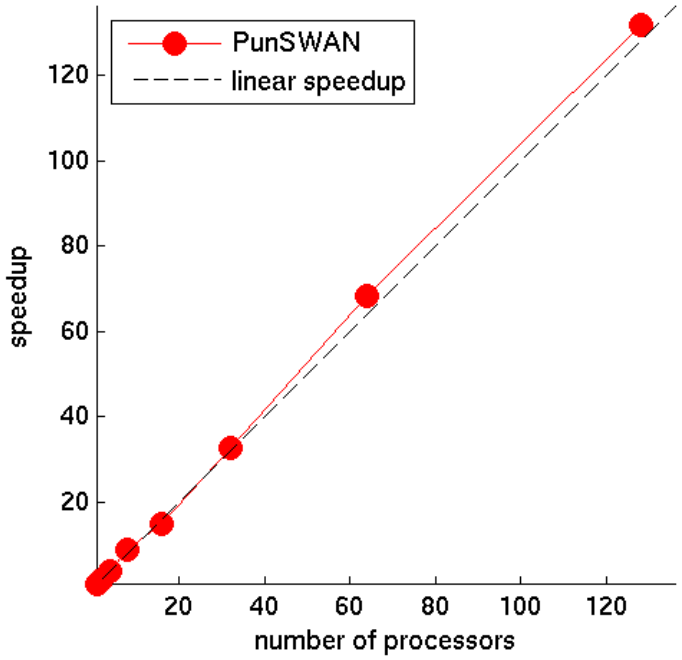

Figure 4: Measured speedups of parallel, unstructured SWAN for the Wadden Sea case on Huygens machine.

The mesh partitioning is designed to uniformly distribute the computational load, i.e. local meshes with a similar number of nodes, and minimise the communications. Note how the local meshes decrease in geographical area as their average mesh size is decreased.

The speedup is defined as the ratio of the computing time for the model running on one processor to the time needed to carry out a run on several processors. With the obtained partition, the speedup is equal to or larger than the number of processors, as illustrated in Fig. 4.

3.2 Selection of storm instants

Three severe westerly storms (wind speeds of 8 to 24ms^{-1}) were observed in the inlet of Ameland during the 2006-2007 winter storm season, namely on 11-12 January 2007, 18-19 January 2007 and 18-19 March 2007. During these events, two arrays of wave buoys were located along transects through the tidal inlet, starting seaward of the ebb-tidal delta and ending well into the shallow interior. The eastern transect follows the main channel (buoys AZB12-AZB62), whereas the western transect crosses the tidal flats (buoys AZB11-AZB61); see Fig. 5.

The travel time of the waves through the considered model area is small compared to the time scale of atmospheric and hydrodynamic conditions, so the simulations were carried out in the stationary mode. A selection of 5 representative time instants was made, around the peak of the storms: 1) January 11, 13h00 (local time), 2) January 11, 22h40, 3) January 18, 14h00, 4) March 18, 10h00 and 5) March 18, 14h40. These cases feature high wind speeds (on average 20ms^{-1}) and very small depths in the Wadden Sea interior (on average 2m). The wind directions of the selected instants remain in the directional sector $230^o - 280^o$ (Nautical convention). The selected cases provide the opportunity to study both penetration of the North Sea waves in the tidal inlet of Ameland and finite depth wave growth over the shallow Wadden Sea interior.

3.3 Bathymetry, water level, current and wind

The bathymetry (Fig. 5) was obtained from detailed measured bathymetric information and interpolated to the employed computational grid.

For each of the selected storm instants, water level and current fields were computed with a circulation model that includes tidal, wind and wave forcing; for details, see Groeneweg et al. (2009). These outputs are interpolated on the unstructured mesh as well.

Spatially uniform winds were applied over the model domain, computed as the average of the wind observations at three stations HBG, TSW and LWO in the Wadden Sea region (Fig. 5).

3.4 Boundary forcing

As westerly wind prevailed over the Wadden Sea region, the wave energy spectrum measured at the offshore station ELD (located west of Wadden Sea in the North Sea) is imposed at the offshore boundary running along west and north side of the model domain.

3.5 Source term settings

In default mode, UnSWAN uses the wind input and whitecapping expressions of Komen et al. (1984), with wind input based on Snyder et al. (1981) and whitecapping based on Hasselmann (1974), together with the Discrete Interaction Approximation (DIA) for quadruplet nonlinear interactions (Hasselmann et al., 1985). Concerning the shallow source terms, the so-called LTA approach of Eldeberky (1996) for modelling triad wave-wave interaction is employed, depth-induced breaking is modelled according to Battjes and Janssen (1978) and bottom friction is based on the JONSWAP formulation (Hasselmann et al., 1973).

It is well-known that physical processes in spectral wave models have definite limitations. Rogers et al. (2003) and Van der Westhuysen et al. (2007) pointed out a number of deficiencies of some source terms of SWAN in simulating wind-sea and swells in ocean and coastal regions. Overall, the wave height is well reproduced by SWAN, but the wave periods, e.g. T_{m01} and T_{m02}, are consistently underestimated. Moreover, SWAN wave spectra show significant deviations from the observed ones.

The use of mean wave number in the default whitecapping formulation of Hasselmann (1974) often results in too high and too low dissipation rates at the lower and higher frequencies, respectively. Consequently, the spectrum is underestimated at the lower frequencies and overestimated at the higher frequencies. This explains the consistent underestimation of the wave periods. Rogers et al. (2003) altered the weight of the relative wave number in the default whitecapping formulation, such that the lower frequencies are more evolved, i.e.

less dissipation rates at those frequencies, and the higher frequencies are less overestimated. They reported significantly better reproduction of the wave periods.

Alternatively, Van der Westhuysen et al. (2007) proposed a saturation-based whitecapping expression based on that of Alves and Banner (2003) in conjunction with a wind input term based on that of Yan (1987). It is demonstrated that this alternative setting yields improved agreement with fetch- and depth-limited growth curves. Also, contrary to the model of Komen et al. (1984), it correctly predicts the wind-sea part of the spectrum under combined swell-sea conditions.

The simulations of Groeneweg et al. (2009) were conducted using the physical settings of Van der Westhuysen et al. (2007) and the DIA for quadruplets. The shallow water source terms have been applied with their default formulations and the corresponding parameter values: bottom friction with coefficient $C_{\mathrm{b}} = 0.067\mathrm{m}^2\mathrm{s}^{-3}$, surf breaking with breaker index $\gamma_{\mathrm{BJ}} = 0.73$, and triad interactions with coefficient $\alpha_{\mathrm{EB}} = 0.05$. In the present study, these settings are regarded as default.

4 Revision of source term settings

Groeneweg et al. (2009) have indicated three main observed inaccuracies in their SWAN hindcasts, two of which will be discussed in the present paper, namely, 1) inaccurate estimation of low-frequency wind-generated wave components in the region of the ebb-tidal delta and 2) underestimation of wave heights and periods under finite depth wave growth conditions in the near-horizontal Wadden Sea interior.

Possible sources of inaccuracies and alternative parameterizations found in the literature for improving the model skill will be discussed in the next two sections. This is followed by summarizing the optimal model settings. No attempt has been made in this study to carry out a calibration process.

4.1 Penetration of North Sea waves

It was shown that most North Sea waves do not penetrate to the main coast in tidal inlets but do penetrate in the more exposed areas. Moreover, it appears that SWAN underestimates the amount of low-frequency peak energy of wind-generated waves that penetrates to the mainland coast. Groeneweg et al. (2009) suggest that this is due to the application of only linear refraction as a propagation mechanism predicting most of the wave energy is trapped on the tidal flats, whereas a small fraction of the energy is propagated across the main tidal channel. However, we believe that the origin of the observed underestimation of the low-frequency wind-sea peak on the ebb-tidal delta cannot be associated with any propagation phenomenon and that the cause must be sought in the SWAN source term settings. Sensitivity analysis showed that the source term of bottom friction has a significant effect on the primary peak of the spectrum.

The default JONSWAP formulation of Hasselmann et al. (1973) models energy dissipation by bottom friction using a tunable friction parameter C_{b}. Hasselmann et al. (1973) found $C_{\mathrm{b}} = 0.038\mathrm{m}^2\mathrm{s}^{-3}$ which is in agreement with the JONSWAP result for swell dissipation. However, Bouws and Komen (1983) suggest a value of $C_{\mathrm{b}} = 0.067\mathrm{m}^2\mathrm{s}^{-3}$ for depth-limited wind-sea conditions in the North Sea. This value is derived from revisiting the energy balance equation employing an alternative deep water dissipation deviated from the one used in SWAN. Since this is the default value used in SWAN, it becomes questionable.

Generally, short waves are much less affected by the bottom friction than long waves. So, it is expected that bottom friction dissipates most of the energy at relative low frequencies. In this paper, we reuse $C_{\mathrm{b}} = 0.038\mathrm{m}^2\mathrm{s}^{-3}$ which is found to be appropriate for swell conditions. We assume, however, that this might also be the case for relative low frequencies in the wind-sea spectrum as well. Hence, we believe that the default SWAN value $C_{\mathrm{b}} = 0.067\mathrm{m}^2\mathrm{s}^{-3}$ is erroneous and will dissipate too much energy at the lower frequencies. Lowering the value of C_{b} (from $0.067\mathrm{m}^2\mathrm{s}^{-3}$ to $0.038\mathrm{m}^2\mathrm{s}^{-3}$) will dissipate less energy at relative low frequencies in both swell and wind-sea parts.

4.2 Finite-depth wave growth

Because of the dominance of locally generated waves in the Wadden Sea interior, the inaccuracy of finite depth wave growth in SWAN affects the reliability of computed wave conditions along the mainland coast of the Netherlands. This inaccuracy can be expressed as a systematic underestimation of the dimensionless ratio H_{m0}/d, with H_{m0} the significant wave height and d the local water depth. The default setting of the source term for depth-induced breaking in SWAN is found to be strong in finite depth growth situations (Groeneweg et al.,

2009; Van der Westhuysen, 2009).

The depth-induced breaking expression of Battjes and Janssen (1978) developed for surf zones and used in SWAN, has proved to be successful in a wide range of situations. Usually, this formulation is studied for the case of waves from deep water breaking on a beach. However, its role in finite depth wave growth has received relatively little attention (Van der Westhuysen, 2009). The main calibration parameter in the formulation of Battjes and Janssen (1978) is the breaker index $\gamma_{\rm BJ}$. Several studies proposed dependencies of $\gamma_{\rm BJ}$ on some local wave characteristics. For example, Ruessink et al. (2003) proposed a dependency of $\gamma_{\rm BJ}$ on the dimensionless depth $k_p\,d$, where k_p is the peak wave number of the wave spectrum,

$$\gamma_{\rm BJ} = 0.76\,k_p\,d + 0.29\,. \qquad (1)$$

This breaker index parameterization is derived for sloping bed surf zones situations. However, Van der Westhuysen (2009) shows that this parameterization also yields optimal values of $\gamma_{\rm BJ}$ for finite depth wave growth over near-horizontal bottoms, including those found in the Wadden Sea interior.

Given the promising results of the Ruessink et al. (2003) parameterization found in the aformentioned study, this formulation is considered suitable for practical application in its present form and will be employed in the present study.

4.3 Optimal model settings

Based on the considerations as outlined in the previous sections, the obtained optimal model settings, to be applied in the present study, are given as follows.

- For the effect of growth and decay of wave energy, the default formulations of Komen et al. (1984) with the modified whitecapping expression of Rogers et al. (2003), so-called n2.0 setting, are adopted. This setting will eliminate problems associated with non-physical dependence of the whitecapping term on mean wave number.

- Four-wave interactions are modelled using the DIA approach of Hasselmann et al. (1985).

- Bottom friction is specified using the JONSWAP formulation with friction parameter $C_{\rm b} = 0.038{\rm m}^2{\rm s}^{-3}$, thus enhancing the predictive ability with respect to the low-frequency part of the wind-sea spectrum.

- The breaker index parameterization of Ruessink et al. (2003) is employed as it will improve finite depth results with Battjes and Janssen (1978) surf breaking significantly.

- The triad wave-wave interaction is omitted for two reasons. Firstly, it is well-known that the LTA approach leads to a significant overestimation of the energy transfer to super-harmonic frequencies, and consequently to a considerable underestimation of the energy level at the primary peak. Secondly, based on an analysis with a newly developed three-wave interaction approximation (Holthuijsen, 2009, private communication), there is an indication that this physical process has a relative minor contribution to the wave dynamics in the shallow parts of the Wadden Sea region.

5 Validation and performance

The simulations for the selected instants were carried out by applying the default source term settings as employed in the hindcast study of Groeneweg et al. (2009) and given in Section 3.5. This was repeated for the optimal model settings as given in Section 4.3. The frequencies ranged from 0.03Hz to 1.0Hz and are distributed on a logarithmic scale into 37 bins, while the directions are divided into 36 sectors of each 10^o. The stationary simulations are solved iteratively and the convergence criteria are based on the so-called curvature-based criteria proposed by Zijlema and Van der Westhuysen (2005). All the simulations were performed using 128 processors on an IBM Power6 cluster (max. 60 Teraflops), Huygens, a new Dutch national supercomputer at the supercomputing center SARA at Amsterdam. Each simulation consumes roughly 5 minutes wall-clock time.

Computed frequency spectra were compared against measurements at all buoy locations. The effect of both default and optimal model settings on spectra were evaluated. Some of these results are highlighted in this paper. Fig. 6 displays a comparison between the predicted and measured wave spectra at buoys AZB21 (Jan. 11, 13h00), AZB31 (Jan. 11, 13h00 and Mar. 18, 10h00) and AZB32 (Mar. 18, 10h00). These buoys are located on the ebb-tidal delta. The systematic underprediction of the wave energy at the primary peak by the default model settings can clearly be observed. This is also reported by Groeneweg et al. (2009). Furthermore, by employing the optimal model settings, the spectra at the lower frequencies are better reproduced. In particular, the energy around the

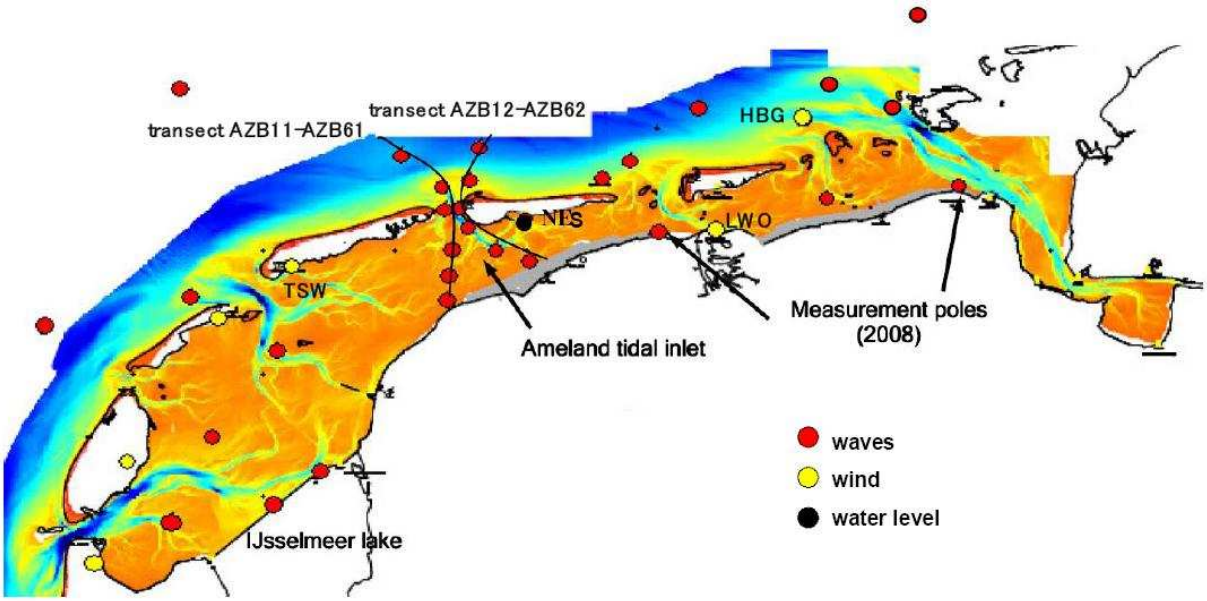

Figure 5: Bathymetry and the locations of the wave buoys in the tidal inlet of Ameland (courtesy of Deltares, The Netherlands).

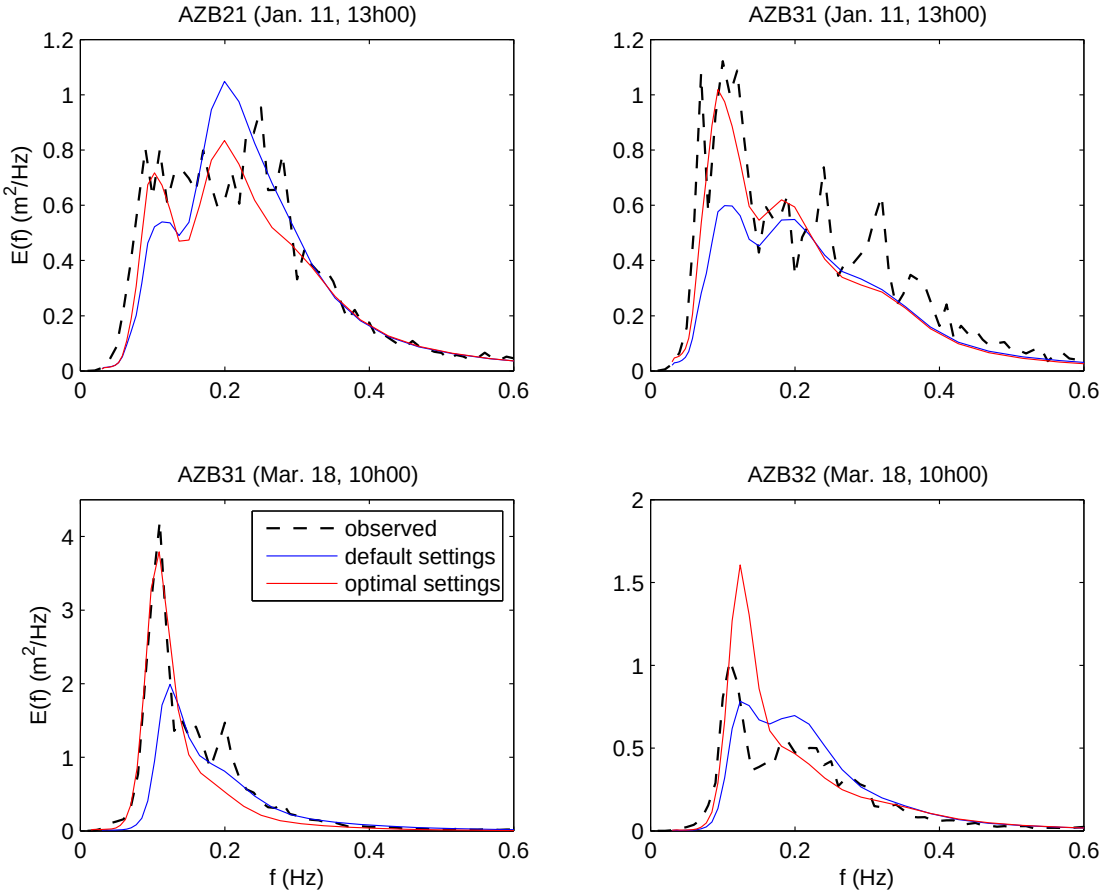

Figure 6: Comparison of simulated and measured spectra at some buoy locations on ebb-tidal delta of Ameland.

lowest peak frequency is significantly improved. Sensitivity analysis showed that this is mainly due to the application of the lowered friction parameter C_{b} in the JONSWAP formulation. Note the variation in scale for the two time instants showed (Jan. 11, 13h00 and Mar. 18, 10h00) at location AZB31.

The predictive skill of the source term settings discussed here was determined by measuring the bias and the scatter index SI. These are given by

$$\mathrm{bias} = \frac{1}{N}\sum_{i=1}^{N}\left(\phi^i_{\mathrm{comp}} - \phi^i_{\mathrm{obs}}\right) \tag{2}$$

and

$$\mathrm{SI} = \frac{\sqrt{\frac{1}{N}\sum_{i=1}^{N}\left(\phi^i_{\mathrm{comp}} - \phi^i_{\mathrm{obs}}\right)^2}}{\frac{1}{N}\sum_{i=1}^{N}\phi^i_{\mathrm{obs}}} \tag{3}$$

where ϕ_{obs} is the observed wave parameter, ϕ_{comp} is the corresponding value computed by UnSWAN and N is the total number of data points in a given data set. These statistical measures were determined for the significant wave height H_{m0}, the peak period T_p and the spectral periods T_{m-10}, T_{m01} and T_{m02}, and were computed for all considered storm instants and available data. The scatter plots and statistical scores are presented in Figs. 7 and 8.

Clearly, the periods computed by the default model settings are systematically lower than the measured values. By contrast, almost no hindcast bias was computed with the optimal model settings for wave periods (Fig. 8). This can be explained to a large extent by the fact that the spectra located at buoys in ebb-tidal delta have relatively more grown at the lower frequencies than at the higher frequencies. As seen earlier, this is a consequence of the use of the lowered parameter C_{b} in the formulation for bottom friction. Both figures also reveal that UnSWAN predicted the wave height very well, no matter what model options were employed.

The scatter indices computed by the optimal settings for T_p, T_{m01} and T_{m02} are slightly larger than those computed by the default ones. However, the opposite is observed for the period T_{m-10}. On the other hand, there is no difference in the scatter index computed by both employed model settings for the wave height. Hence, we may conclude that the reliability of the optimal settings used for the prediction of wave height and periods is very similar to that of default options. In so far, the statistical scores clearly justify the superiority of application of the optimal model settings for the prediction of wave height and periods.

The statistical results for the wave height presented above suggest no improvement of the model outcomes regardless of the model options used. Concerning the finite depth wave growth in the Wadden Sea interior, the buoys AZB41, AZB51, AZB61 and AZB62 were considered separately. Fig. 9 compares the scatter plot results between model and observations for this subset obtained with the default and optimal model settings, respectively. It can be seen that the optimal model options yield a significant improvement in H_{m0}/d ratio over the default ones. Accordingly, the Battjes and Janssen surf breaking source term with the breaker index of Ruessink et al. (2003) improves the prediction of wave heights over nearly horizontal beds. This is also reflected in the wave spectrum as demonstrated in Fig. 10, showing the computed and measured spectra at locations AZB61 (Jan. 18, 14h00) and AZB62 (Jan. 11, 13h00).

6 Summary and conclusion

In this paper, we have presented the set-up, optimization and validation of a highly-resolved, unstructured-mesh SWAN (UnSWAN) model for the Dutch Wadden Sea. Although the present work has to be considered as a first attempt towards a high-resolution model of the Wadden Sea, it now appears possible to broaden the range of scales simulated by a single model.

Performance of UnSWAN was investigated using the wave measurements during three severe storms of 2007 in the tidal inlet of Ameland. Using the optimal model settings discussed in this paper, UnSWAN is skillful in predicting the variations of wave height and periods in the tidal inlet, over the ebb-tidal delta and over the shallow Wadden Sea interior.

Our experiences to date with simulating storm events in the Wadden Sea indicate that improvements in spectral wave modeling, including optimization of the UnSWAN source term settings, and in domain definition and mesh resolution, significantly increases the accuracy and reliability of SWAN. Moreover, high-performance computing with unstructured meshes opens the possibility to simulating storms at unprecedented fidelity and gives rise to a number of modeling challenges.

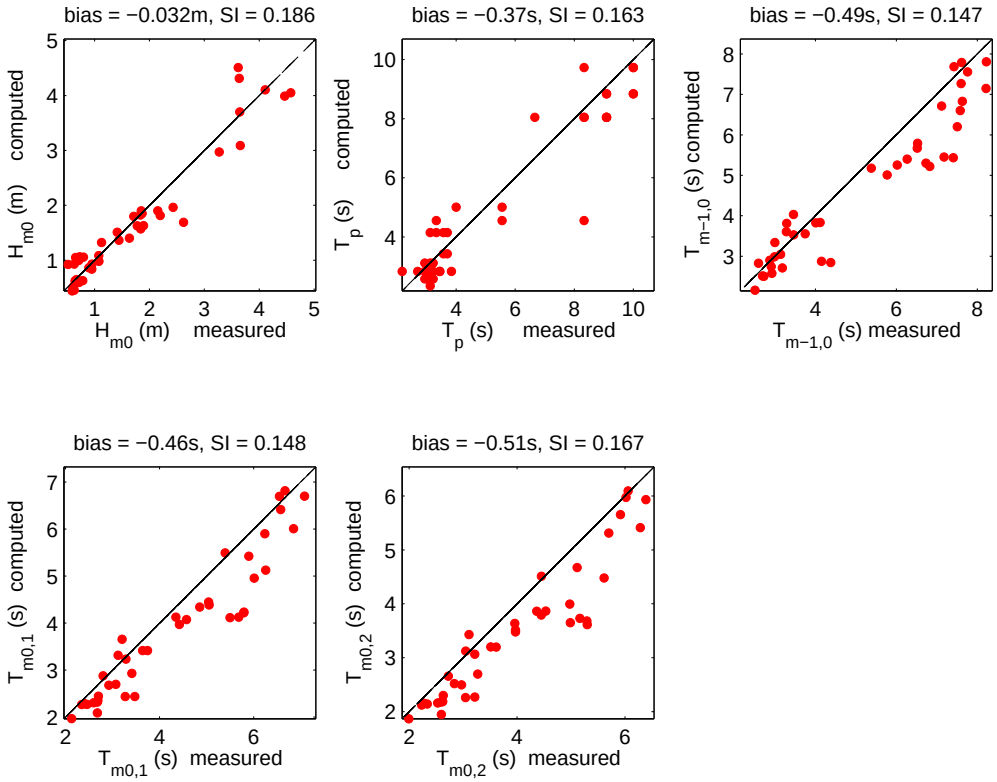

Figure 7: Scatter plots of computed and observed wave parameters with default model settings.

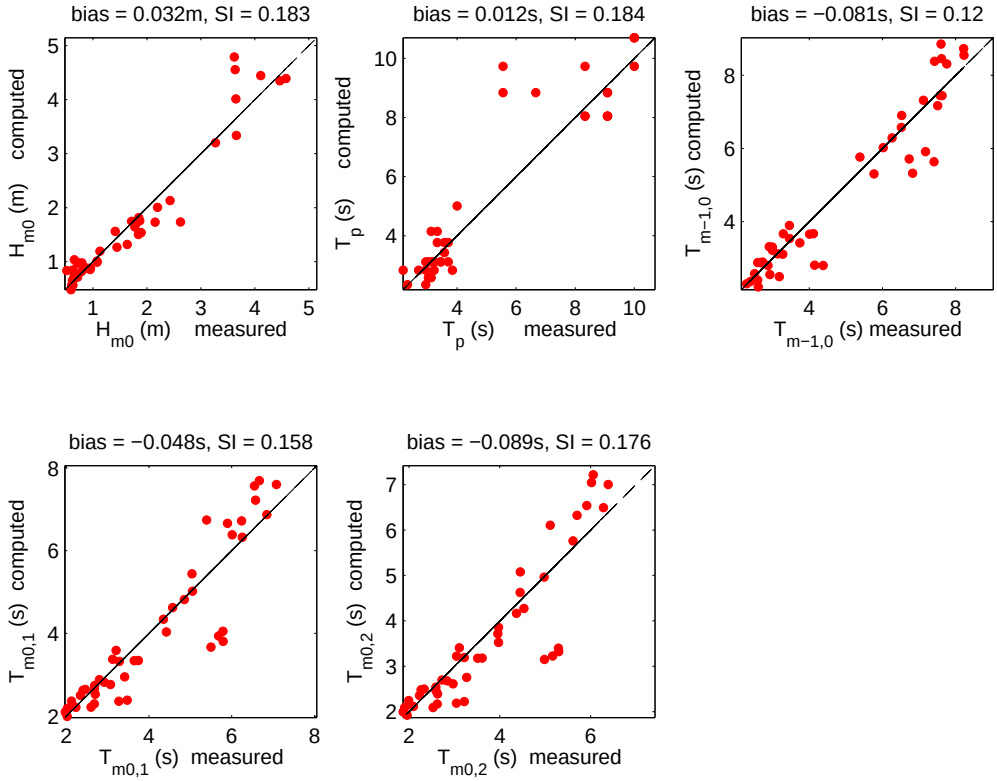

Figure 8: Scatter plots of computed and observed wave parameters with optimal model settings.

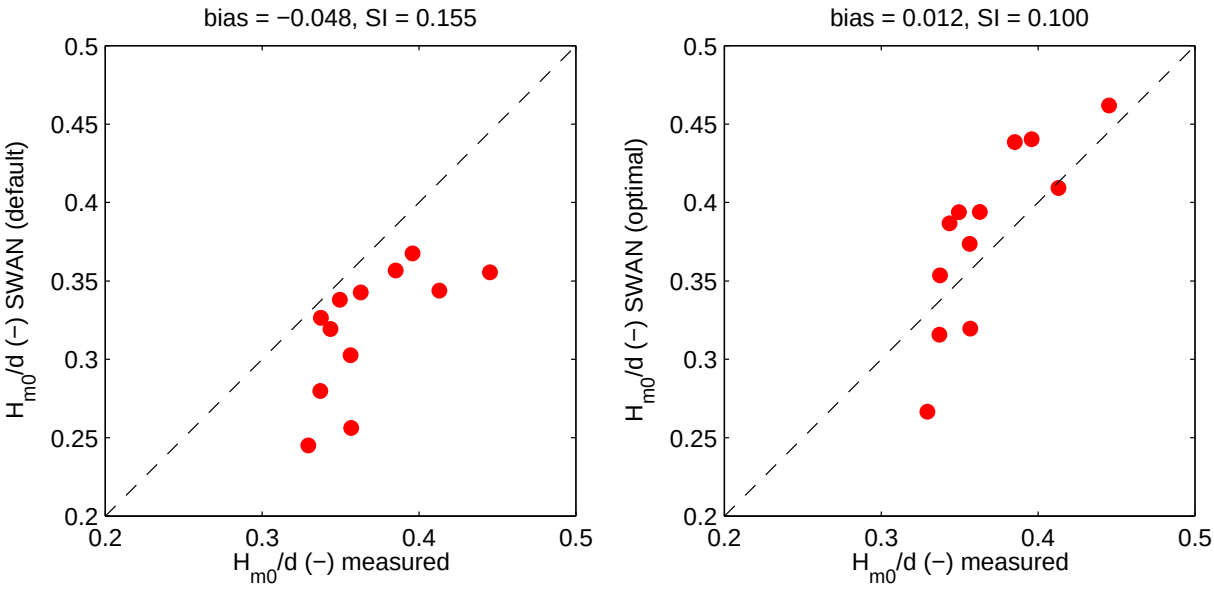

Figure 9: Scatter plots of computed and observed H_{m0}/d ratio at locations AZB41, AZB51, AZB61 and AZB62 with default (left panel) and optimal (right panel) model settings.

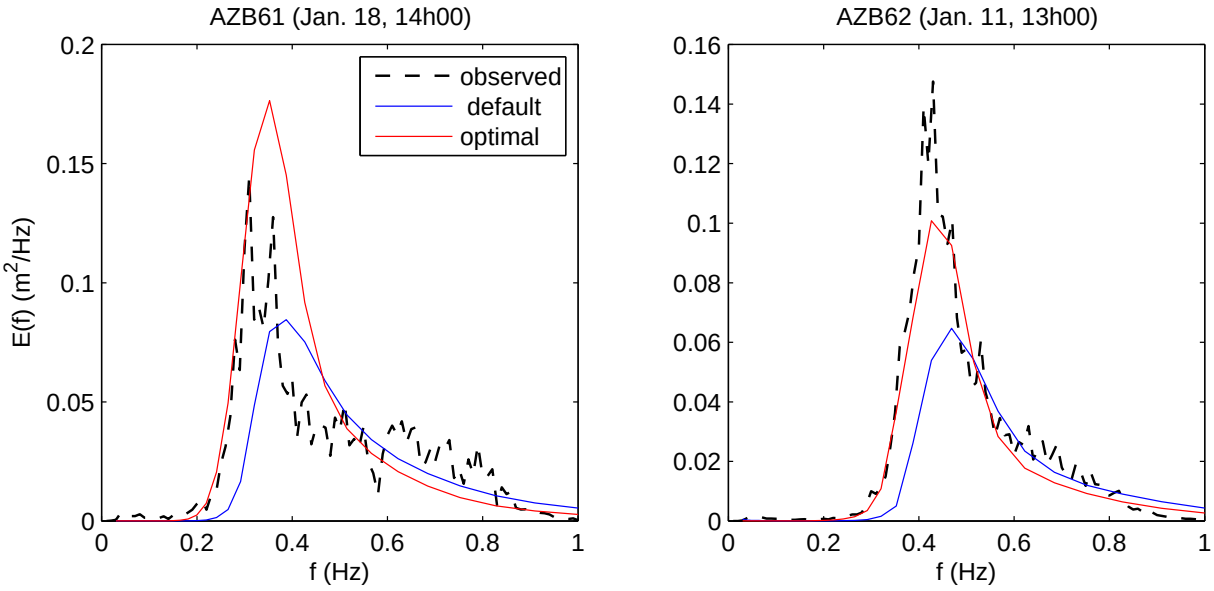

Figure 10: Comparison of simulated and measured spectra at locations AZB61 and AZB62 on tidal flats.

Acknowledgements

Part of this work was sponsored by the National Computing Facilities Foundation (NCF) for the use of supercomputer facilities, with financial support from the Netherlands Organization for Scientific Research (NWO). Gerbrant van Vledder, André van der Westhuysen, Ivo Wenneker and Jacco Groeneweg are acknowledged for their input.

References

Alves, J.H.G.M. and M.L. Banner, 2003: Performance of a saturation-based dissipation-rate source term in modelling the fetch-limited evolution of wind waves. *Journal of Physical Oceanography*, **33**, 1274–1298.

Battjes, J.A. and J.P.F.M. Janssen, 1978: Energy loss and set-up due to breaking of random waves. *Proceedings 16th International Conference on Coastal Engineering*, pp. 569–587.

Bilgili, A. and K.W. Smith, 2003: BatTri: a 2-D finite element grid generator, version 11.11.03. Available from: <http://www-nml.dartmouth.edu/Publications/internal_reports/NML-03-15/>.

Booij, N., R.C. Ris and L.H. Holthuijsen, 1999: A third-generation wave model for coastal regions, 1. Model description and validation. *Journal of Geophysical Research*, **104**, C4, 7649–7666.

Bouws, E. and G.J. Komen, 1983: On the balance between growth and dissipation in an extreme depth-limited wind-sea in the southern North Sea. *Journal of Physical Oceanography*, **13**, 1653–1658.

Eldeberky, Y., 1996: Nonlinear transformation of wave spectra in the nearshore zone. Ph.D. thesis, Delft University of Technology, Delft, The Netherlands.

Groeneweg, J., A. van der Westhuysen, G. van Vledder, S. Jacobse, J. Lansen and A. van Dongeren, 2009: Wave modelling in a tidal inlet: performance of SWAN in the Wadden Sea. *Proceedings 31th International Conference on Coastal Engineering*, pp. 411–423.

Hasselmann, K., T.P. Barnett, E. Bouws, H. Carlson, D.E. Cartwright, K. Enke, J.A. Ewing, H. Gienapp, D.E. Hasselmann, P. Kruseman, A. Meerburg, O. Müller, D.J. Olbers, K. Richter, W. Sell and H. Walden, 1973: Measurements of wind-wave growth and swell decay during the Joint North Sea Wave Project (JONSWAP). Dtsch. Hydrogr. Z., Suppl. 12, **A8**, 95 pp.

Hasselmann, K., 1974: On the spectral dissipation of ocean waves due to white capping. *Boundary-Layer Meteorology*, **6**, 107–127.

Hasselmann, S., K. Hasselmann, J.H. Allender and T.P. Barnett, 1985: Computations and parameterizations of the nonlinear energy transfer in a gravity wave spectrum. Part II: parameterizations of the nonlinear transfer for application in wave models. *Journal of Physical Oceanography*, **15**, 1378–1391.

Karypis, G. and V. Kumar, 1998: METIS: family of multilevel partitioning algorithms. Available from: <http://glaros.dtc.umn.edu/gkhome/views/metis>.

Komen, G.J., S. Hasselmann and K. Hasselmann 1984: On the existence of a fully developed wind-sea spectrum. *Journal of Physical Oceanography*, **14**, 1271–1285.

Ris, R.C., L.H. Holthuijsen, J.M. Smith, N. Booij and A.R. van Dongeren, 2002: The ONR Test Bed for coastal and oceanic wave models. *Proceedings 28th International Conference on Coastal Engineering*, pp. 380–391.

Rogers, W.E., P.A. Hwang and D.W. Wang, 2003: Investigation of wave growth and decay in the SWAN model: three regional-scale applications. *Journal of Physical Oceanography*, **33**, 366–389.

Ruessink, B.G., D.J.R. Walstra and H.N. Southgate, 2003: Calibration and verification of a parametric wave model on barred beaches. *Coastal Engineering*, **48**, 139–149.

Snyder, R.L., F.W. Dobson, J.A. Elliott and R.B. Long, 1981: Array measurements of atmospheric pressure fluctuations above surface gravity waves. *Journal of Fluid Mechanics*, **102**, 1–59.

Van Vledder, G.P., J. Groeneweg and A.J. van der Westhuysen, 2009: Numerical and physical aspects of wave modelling in a tidal inlet. *Proceedings 31th International Conference on Coastal Engineering*, pp. 424–436.

Van der Westhuysen, A.J., M. Zijlema and J.A. Battjes, 2007: Nonlinear saturation-based whitecapping dissipation in SWAN for deep and shallow water. *Coastal Engineering*, **54**, 151–170.

Van der Westhuysen, A.J., 2009: Modelling of depth-induced wave breaking under finite-depth wave growth

conditions. *Journal of Geophysical Research*, in review.

Westerink, J.J., R.A. Luettich, J.C. Feyen, J.H. Atkinson, C. Dawson, H.J. Roberts, M.D. Powell, J.P. Dunion, E.J. Kubatko and H. Pourtaheri, 2008: A basin to channel scale unstructured grid hurricane storm surge model applied to Southern Louisiana. *Monthly Weather Review*, **136**, 833–864.

Yan, L., 1987: An improved wind input source term for third generation ocean wave modelling. Rep. 87-8, Royal Dutch Meteor. Inst., 20 pp.

Zijlema, M. and A.J. van der Westhuysen, 2005: On convergence behaviour and numerical accuracy in stationary SWAN simulations of nearshore wind wave spectra. *Coastal Engineering*, **52**, 237–256.

Zijlema, M., 2009: Parallel, unstructured mesh implementation for SWAN. *Proceedings 31th International Conference on Coastal Engineering*, pp. 470–482.